Available online at www.sciencedirect.com
ScienceDirect
Nuclear Physics B Proceedings Supplement 00 (2012) 1–6
Nuclear Physics B Proceedings Supplement

Measurements of semileptonic mixing asymmetries for B^0 and B_s^0 mesons

M. R. J. Williams (on behalf of the D0 Collaboration)

Lancaster University, UK LA1 4YB

Abstract

We present measurements of the semileptonic mixing asymmetries for $B^0_{(s)}$ mesons, $a^{d(s)}_{\rm sl}$, using a data sample corresponding to 10.4 fb^{-1} of $p\bar{p}$ collisions at $\sqrt{s} = 1.96$ TeV, collected with the D0 experiment at the Fermilab Tevatron collider. For the $a^d_{\rm sl}$ measurement, two independent decay channels are used: $B^0 \to \mu^+ D^- X$, with $D^- \to K^+\pi^-\pi^-$; and $B^0 \to \mu^+ D^{*-} X$, with $D^{*-} \to \bar{D}^0\pi^-$, $\bar{D}^0 \to K^+\pi^-$. For the $a^s_{\rm sl}$ measurement, the channel $B^0_s \to \mu^+ D_s^- X$, with $D_s^- \to \phi\pi^-$, $\phi \to K^+K^-$ is used. For each channel, we extract the raw charge asymmetries, correct for detector-related asymmetries using data-driven methods, and account for dilution from charge-symmetric processes using Monte Carlo simulation. The final $a^d_{\rm sl}$ measurement combines four visible proper decay length regions for each channel, yielding $a^d_{\rm sl} = [0.68 \pm 0.45\ (\text{stat.}) \pm 0.14\ (\text{syst.})]\%$. This is the single most precise measurement of this parameter, with uncertainties smaller than the current world average of B factory measurements. Using the B^0_s meson sample, we make a single time-integrated measurement, $a^s_{\rm sl} = [-1.12 \pm 0.74\ (\text{stat.}) \pm 0.17\ (\text{syst.})]\%$. Both measurements are in agreement with the standard model predictions.

Keywords: B meson oscillation, charge asymmetry, CP violation

1. Introduction

It is a long standing puzzle that the current matter-dominance of the universe cannot be explained by the particle interactions described in the standard model (SM) of particle physics alone. One necessary ingredient to drive such an asymmetry is the violation of CP symmetry (CPV) [1]. Certain SM processes indeed satisfy this requirement, as a result of the complex phase in the quark mixing matrix of the weak interaction [2]; however, their effects are too weak to explain the matter dominance [3]. As such, it is important to search for further non-SM sources of CPV.

Studies of neutral B meson oscillations, whereby a neutral meson changes into its own antiparticle via a box-diagram-mediated weak interaction [2], provide a sensitive probe for such CPV processes. The semileptonic mixing asymmetry, defined as:

$$a^q_{\rm sl} = \frac{\Gamma(\bar{B}^0_q \to B^0_q \to \ell^+ X) - \Gamma(B^0_q \to \bar{B}^0_q \to \ell^- X)}{\Gamma(\bar{B}^0_q \to B^0_q \to \ell^+ X) + \Gamma(B^0_q \to \bar{B}^0_q \to \ell^- X)}, \quad (1)$$

allows the effects of any CP-violating processes to be directly observed in terms of the resulting asymmetry of the decay products. Here ℓ denotes a charged lepton of any flavor, and q represents the flavor of the non-b valence quark of the meson.

In the standard model, the semileptonic mixing asymmetry is related to the properties of the corresponding B meson system, namely the mass difference $\Delta M_q = M(B^0_{qH}) - M(B^0_{qL})$, the decay-width difference $\Delta\Gamma_q = \Gamma(B^0_{qL}) - \Gamma(B^0_{qH})$, and the CP-violating phase ϕ_q, by:

$$a^q_{\rm sl} = \frac{|\Gamma^q_{12}|}{|M^q_{12}|}\sin\phi_q = \frac{\Delta\Gamma_q}{\Delta M_q}\tan\phi_q. \quad (2)$$

Here the states B^0_{qH} and B^0_{qL} are the heavy and light mass eigenstates of the B meson system, which differ from the flavor eigenstates. M^q_{12} and Γ^q_{12} are respectively the off-diagonal elements of the mass and decay matrices [2].

The standard model predictions [4] for both $a^s_{\rm sl}$ and

$a^d_{\rm sl}$ are very small:

$$a^d_{\rm sl} = (-0.041 \pm 0.006)\%, \quad (3)$$
$$a^s_{\rm sl} = (0.0019 \pm 0.0003)\%. \quad (4)$$

These predictions are effectively negligible compared to the current experimental precision. Hence, the measurement of any significant deviation from zero is an unambiguous signal of new physics, which could lead to order-of-magnitude enhancements of $|a^d_{\rm sl}|$ [5].

The B^0 semileptonic mixing asymmetry, $a^d_{\rm sl}$, has been extensively studied by the B factories operating at the $\Upsilon(4S)$ resonance. The current world average of these measurements is [2]:

$$a^d_{\rm sl} = (-0.05 \pm 0.56)\%. \quad (5)$$

The most precise published measurement of $a^s_{\rm sl}$ was performed by the D0 Collaboration [6],

$$a^s_{\rm sl} = [-0.17 \pm 0.91\ (\text{stat.})\ ^{+0.12}_{-0.23}\ (\text{syst.})]\%. \quad (6)$$

The recent evidence for a non-zero dimuon charge asymmetry by the D0 experiment is sensitive to the linear combination of B^0 and B^0_s mixing asymmetries, with approximately equal contributions from each source [7]. The measurement constrains a band in the $(a^d_{\rm sl}, a^s_{\rm sl})$ plane, which is inconsistent with the SM prediction at the 3.9 standard deviations level. On the other hand, recent searches for CPV in $B^0_s \to J/\psi\phi$ decays from the D0 [8], CDF [9], and LHCb [10] collaborations find agreement of the CP-violating phase ϕ_s with SM predictions. Given the current body of experimental evidence, improved measurements of both $a^d_{\rm sl}$ and $a^s_{\rm sl}$ are required in order to constrain the possible sources of new physics in B meson mixing and decay [11].

2. Overview

For the B^0 meson case, two separate decay channels are used:

1. $B^0 \to \mu^+\nu D^- X$,
   with $D^- \to K^+\pi^-\pi^-$
   (plus charge conjugate process);
2. $B^0 \to \mu^+\nu D^{*-} X$,
   with $D^{*-} \to \bar{D}^0\pi^-, \bar{D}^0 \to K^+\pi^-$
   (plus charge conjugate process);

The two channels are treated separately, with each being used to extract $a^d_{\rm sl}$, before the final measurements are combined.

For the B^0_s measurement, a single channel is used:

1. $B^0_s \to \mu^+\nu D^-_s X$,
   with $D^-_s \to \phi\pi^-, \phi \to K^+K^-$
   (plus charge conjugate process);

For clarity, the charges are henceforward only included where necessary to avoid ambiguity, and the three channels are denoted by μD, μD^*, and μD_s respectively.

Experimentally, the semileptonic mixing asymmetries can be expressed in the following form:

$$a^q_{\rm sl} = \frac{A - A_{\rm BG}}{F^{\rm osc}_{B_{(s)}}}. \quad (7)$$

Here, A is the measured raw asymmetry, defined by:

$$A = \frac{N_{\mu^+ D^{(*)-}_{(s)}} - N_{\mu^- D^{(*)+}_{(s)}}}{N_{\mu^+ D^{(*)-}_{(s)}} + N_{\mu^- D^{(*)+}_{(s)}}} \equiv \frac{N_{\rm diff}}{N_{\rm sum}}, \quad (8)$$

where $N_{\mu^\pm D^{(*)\mp}_{(s)}}$ is the number of reconstructed $\mu^\pm D^{(*)\mp}_{(s)}$ signal candidates. The term $A_{\rm BG}$ accounts for inherent detector-related background asymmetries, for example due to the different reconstruction efficiencies for positively and negatively charged kaons. The denominator $F^{\rm osc}_{B_{(s)}}$ is defined as the fraction of all $\mu D^{(*)}_{(s)}$ signal events that arise from decays of $B^0_{(s)}$ mesons after they have oscillated. All background asymmetries are extracted using data-driven methods, while Monte Carlo (MC) simulation is used to determine the fraction of $B^0_{(s)}$ mesons that have undergone mixing prior to decay.

The B^0 meson has a mixing frequency $\Delta M_d = 0.507 \pm 0.004\ \text{ps}^{-1}$, of comparable scale to the lifetime $\tau(B^0) = 1.518 \pm 0.007$ ps [2]. Hence the fraction of oscillated B^0 mesons is a strong function of the measured decay time. As such, the extraction of $a^d_{\rm sl}$ is performed in six regions of visible proper decay length (VPDL), where

$$\text{VPDL}(B) = L_{xy}(B) \cdot \frac{cM(B)}{p_T(\mu D)}. \quad (9)$$

Here, L_{xy} is the decay length of the B^0 meson in the transverse plane. The selected VPDL(B^0) bins are defined by the edges {−0.10, 0.00, 0.02, 0.05, 0.10, 0.20, 0.60} cm. The first two bins have negligible contributions from oscillated B^0 mesons, and are not included in the final $a^d_{\rm sl}$ measurement. They represent a control region in which the measured raw asymmetry should be dominated by the background contribution, i.e., $A - A_{\rm BG} \approx 0$.

In contrast, the mixing frequency of the B^0_s meson is much higher, $\Delta M_s = 17.69 \pm 0.08\ \text{ps}^{-1}$, resulting in a dilution $F^{\rm osc}_{B_s}$ which is consistently around 50% for all measured decay times. In this case, a single time-integrated measurement is performed, without division into VPDL(B^0_s) bins.

3. The D0 Detector

The D0 detector has been described in detail elsewhere [12]. The most important detector components for these measurements are the central tracking system, the muon detectors, and the magnets. The central tracking system comprises a silicon microstrip tracker and a central fiber tracker, both located within a 2 T superconducting solenoidal magnet. A muon system resides beyond the calorimeter, and consists of a layer of tracking detectors and scintillation trigger counters before a 1.8 T toroidal magnet, followed by two similar layers after the toroid.

The polarities of both the solenoidal and toroidal magnets were regularly reversed during data acquisition, approximately every two weeks, resulting in almost equal beam exposure in each of the four polarity configurations. This feature of the D0 detector is crucial in reducing detector-related asymmetries, for example due to the different trajectories of positive and negative muons as they traverse the magnetic fields in the detector.

4. Event Selection

The measurements presented here use data collected by the D0 detector from 2002–2011, corresponding to $\sim$10.4 fb^{-1} of integrated luminosity, and representing the full Tevatron Run II sample of $p\bar{p}$ collisions at center-of-mass energy $\sqrt{s}$ = 1.96 TeV. Signal candidates are collected using single and dimuon triggers. To avoid lifetime-dependent trigger efficiencies, which are difficult to model in simulation, events that exclusively satisfy muon triggers with track impact-parameter requirements are removed.

For all three channels, events are considered for selection if they contain a muon candidate passing tight quality requirements, and matched to a track in the central tracking system. The muon must have transverse momentum $p_T > 2$ GeV/c, and total momentum $p > 3$ GeV/c.

For events fulfilling these requirements, $D^{(*)}_{(s)}$ candidates are constructed by combining three other tracks associated with the same initial $p\bar{p}$ interaction. Each track must satisfy $p_T > 0.7$ GeV/c, and the resulting $D^{(*)}_{(s)}$ candidate must be consistent with originating from a common vertex with the muon. The $\mu D_{(s)}$ candidates must have an invariant mass consistent with the expectations from $B^0_{(s)}$ decay. Additional loose reconstruction requirements are applied to limit the combinatorial backgrounds at this preselection stage.

The final event selections utilize channel-specific multivariate discriminants, which combine several variables into a single parameter with improved ability to separate signal (S) and background (B) events. The multivariate discriminants are optimised using Monte Carlo (MC) simulation to model the signal, and sideband regions in data to model the background.

The final choice of cuts are selected to maximise the signal significance $N_S / \sqrt{N_S + N_B}$ of the $D^{(*)}_{(s)}$ peaks, as determined from a small sub-set of the data. For the B^0 case, the cuts are optimized separately in each VPDL bin, taking advantage of the diminishing background at larger values to improve the signal efficiency and significantly improve the final precision on $a^d_{\rm sl}$.

5. Event Weights

In any given configuration of the solenoidal and toroidal magnet polarities, there can be detector-related asymmetries. These originate from differing detection efficiencies for positively and negatively charged particles, in turn caused by their different trajectories as they bend through the magnetic fields in the detector. The regular reversal of both magnet polarities suppresses such effects. To ensure maximal cancellation of these instrumental asymmetries, an additional event-by-event weighting is applied such that the sums of weights in each (solenoid,toroid) configuration are the same, for a given sample.

This procedure is performed separately for each channel, and for each VPDL bin in the B^0 case. Event weights are typically in the range 0.90–1.00, with very little variation between VPDL bins. The total signal yields after event weighting are $N(\mu D) = 721\,519 \pm 3537$, $N(\mu D^*) = 519\,066 \pm 3446$, and $N(\mu D_s) = 203\,513 \pm 1337$.

6. Extracting the Raw Asymmetry

The raw asymmetry is extracted by fitting the invariant mass distributions: $M(K\pi\pi)$ for the μD candidates, $[\Delta M \equiv M(D^0\pi) - M(D^0)]$ for the μD^* candidates, and $M(\phi\pi)$ for the μD_s candidates. The sum distribution $H_{\rm sum}$ is constructed by weighting all $\mu D^{(*)}_{(s)}$ candidates according to the magnet polarity weight. A difference distribution $H_{\rm diff}$ is constructed by taking the difference betwen the $\mu^+ D^{(*)-}_{(s)}$ and $\mu^- D^{(*)+}_{(s)}$ distributions. The sum and difference distributions are modeled by, respectively, the functions:

$$F_{\rm sum} = F^{\rm BG}_{\rm sum} + N_{\rm sum} \cdot F^{\rm sig}, \quad (10)$$

$$F_{\rm diff} = F^{\rm BG}_{\rm diff} + A \cdot N_{\rm sum} \cdot F^{\rm sig}, \quad (11)$$

where $N_{\rm sum}$ is the total $\mu D^{(*)}_{(s)}$ yield, and A is the corresponding raw charge asymmetry defined in Eq. (8). Different models are used to parametrize the backgrounds for the sum ($F^{\rm BG}_{\rm sum}$) and difference ($F^{\rm BG}_{\rm diff}$) histograms, while a single model $F^{\rm sig}$ is used for the signal in both cases. The yields, asymmetries, and signal and background parameters in these models are extracted by a simultaneous binned fit to the two distributions, to minimise the total χ^2 with respect to the fitting functions. The specific details of the fitting models for the three channels can be found elsewhere [13, 14].

Figure 1 shows an example of the sum and difference fits for the μD^* channel, in the region $(0.10 < {\rm VPDL}(B^0) < 0.20)$ cm. The results for all six VPDL regions, for both B^0 channels, are listed in Table 1. For the B^0_s case, a single raw asymmetry is obtained, $A = [-0.40 \pm 0.33\,({\rm stat.}) \pm 0.05\,({\rm syst.})]\%$. Systematic uncertainties are assigned to account for the choice of bin width, fitting limits, and signal and background models. Charge-randomised ensemble tests demonstrate that the extraction of the raw asymmetries is unbiased and provides accurate uncertainties.

7. Accounting for Detector Asymmetries

In relating the measured raw asymmetry to the physical asymmetry under investigation, the effects of possible charge asymmetries in particle reconstruction must be considered. Neglecting asymmetries of second order or higher, the background asymmetry for both B^0 channels (which contain the same final-state particles $\mu^\pm K^\pm \pi^\mp \pi^\mp$) simplifies to:

$$A_{\rm BG}(B^0) = a^\mu + a^K - 2a^\pi. \quad (12)$$

where the asymmetries a^X are defined as the difference in reconstruction efficiency for the positively and negatively charged particles. The equivalent correction for the B^0_s case is:

$$A_{\rm BG}(B^0_s) = a^\mu + a^\phi - a^\pi. \quad (13)$$

By far the largest background asymmetry to be taken into account is due to differences in the behavior of positive and negative kaons as they traverse the detector. Negative kaons can interact with matter in the tracking system to produce hyperons, while there is no equivelent interaction for positive kaons. The kaon asymmetry is measured using a dedicated sample of $K^{*0} \to K^+\pi^-$ decays, based on the technique described in Ref. [15]. As expected, an overall positive kaon asymmetry is observed, of approximately 1%. A strong dependence on kaon momentum and absolute pseudorapidity is found,

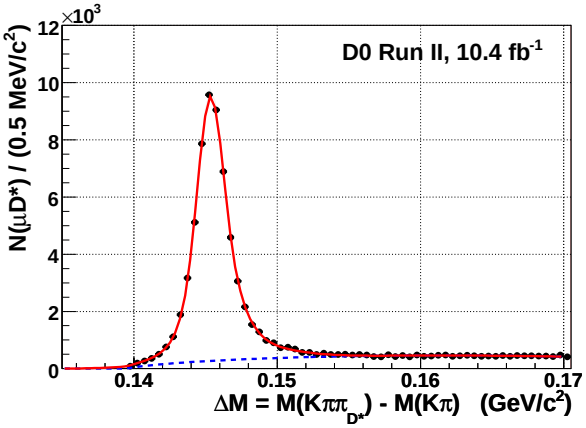

(a) $H_{\rm sum}$

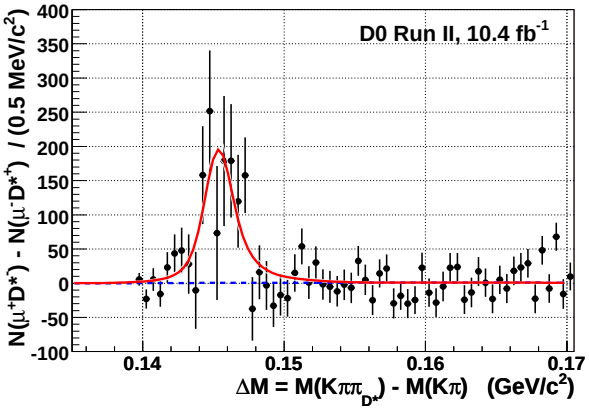

(b) $H_{\rm diff}$

Figure 1: Examples of the raw asymmetry fit for the μD^* channels, for the fifth VPDL(B^0) bin corresponding to $(0.10 < {\rm VPDL}(B^0) < 0.20)$ cm. In both cases, the solid line represents the total fit function, with the background part shown separately by the dashed line.

and hence the final kaon asymmetry correction is determined by the weighted average of $a^K[p(K), |\eta(K)|]$ over the $p(K)$ and $|\eta(K)|$ distributions in the signal events. The resulting corrections a^K are listed in Table 1.

For the B^0_s case, the kaon reconstruction asymmetry cancels almost exactly, except for a slight residual effect caused by interference between the ϕ and $f_0(980)$ which leads to slightly different momentum distributions for the two kaons. The final correction to the raw B^0_s asymmetry from this $\phi \to K^+K^-$ asymmetry is $a^\phi = (+0.020 \pm 0.002)\%$.

The residual charge asymmetry for muon identification is measured using $J/\psi \to \mu^+\mu^-$ decays, using the technique developed in Ref. [15]. A small but significant asymmetry is observed, with a sizeable dependence on the muon transverse momentum. The corresponding corrections a^μ to be applied to the raw asymmetries are

Table 1: The results of the asymmetry extraction, in bins of VPDL(B^0), for both B^0 signal channels. Shown are the raw asymmetries A, the kaon and muon reconstruction asymmetries, the background corrected asymmetries $A_{\rm phys} = A - A_{\rm BG}$, the oscillation fractions $F^{\rm osc}_{B^0}$, and the final measurements of $a^d_{\rm sl}$. In each case, the upper uncertainty is statistical, the lower systematic.

	Bin 1 −0.10 – 0.00 cm	Bin 2 0.00 – 0.02 cm	Bin 3 0.02 – 0.05 cm	Bin 4 0.05 – 0.10 cm	Bin 5 0.10 – 0.20 cm	Bin 6 0.20 – 0.60 cm
μD channel						
A (%)	2.70 ± 1.28 ± 0.19	1.02 ± 0.35 ± 0.07	1.16 ± 0.32 ± 0.08	1.50 ± 0.33 ± 0.07	1.48 ± 0.41 ± 0.05	1.20 ± 0.88 ± 0.13
a^K (%)	1.128 ± 0.041 ± 0.014	1.124 ± 0.040 ± 0.014	1.141 ± 0.040 ± 0.014	1.147 ± 0.040 ± 0.014	1.157 ± 0.040 ± 0.015	1.157 ± 0.040 ± 0.014
a^μ (%)	0.102 ± 0.025 ± 0.008	0.105 ± 0.027 ± 0.009	0.107 ± 0.029 ± 0.012	0.107 ± 0.029 ± 0.013	0.108 ± 0.028 ± 0.011	0.108 ± 0.028 ± 0.009
$A_{\rm phys}$ (%)	1.48 ± 1.28 ± 0.20	−0.20 ± 0.35 ± 0.09	−0.07 ± 0.32 ± 0.10	0.26 ± 0.33 ± 0.09	0.23 ± 0.41 ± 0.07	−0.05 ± 0.89 ± 0.14
$F^{\rm osc}_{B^0}$	0.018 ± 0.003 ± 0.001	0.009 ± 0.001 ± 0.000	0.057 ± 0.002 ± 0.001	0.208 ± 0.003 ± 0.005	0.520 ± 0.005 ± 0.011	0.658 ± 0.010 ± 0.017
$a^d_{\rm sl}$ (%)	Not used		−1.29 ± 5.68 ± 1.69	1.25 ± 1.61 ± 0.43	0.44 ± 0.79 ± 0.14	-0.07 ± 1.36 ± 0.21
μD^* channel						
A (%)	1.82 ± 0.67 ± 0.13	1.10 ± 0.30 ± 0.04	0.94 ± 0.30 ± 0.05	1.38 ± 0.33 ± 0.07	2.11 ± 0.44 ± 0.08	0.55 ± 0.99 ± 0.09
a^K (%)	1.089 ± 0.047 ± 0.013	1.078 ± 0.052 ± 0.014	1.078 ± 0.050 ± 0.014	1.085 ± 0.050 ± 0.014	1.086 ± 0.049 ± 0.014	1.098 ± 0.050 ± 0.014
a^μ (%)	0.097 ± 0.027 ± 0.012	0.098 ± 0.031 ± 0.022	0.101 ± 0.033 ± 0.023	0.101 ± 0.033 ± 0.022	0.101 ± 0.033 ± 0.020	0.101 ± 0.031 ± 0.016
$A_{\rm phys}$ (%)	0.64 ± 0.67 ± 0.14	−0.07 ± 0.31 ± 0.07	−0.23 ± 0.31 ± 0.08	0.20 ± 0.34 ± 0.09	0.93 ± 0.44 ± 0.10	−0.63 ± 0.99 ± 0.11
$F^{\rm osc}_{B^0}$	0.013 ± 0.002 ± 0.001	0.010 ± 0.001 ± 0.000	0.061 ± 0.003 ± 0.002	0.231 ± 0.005 ± 0.003	0.570 ± 0.008 ± 0.007	0.713 ± 0.016 ± 0.008
$a^d_{\rm sl}$ (%)	Not used		−3.79 ± 5.00 ± 1.27	0.87 ± 1.45 ± 0.39	1.63 ± 0.78 ± 0.17	−0.89 ± 1.39 ± 0.15

extracted using the same method as for the kaon asymmetry, by performing a weighted average of the muon asymmetry over bins of $p_T(\mu)$. The final B^0 muon asymmetry corrections for each VPDL bin and both channels are summarized in Table 1. For the B^0_s measurement, the single muon correction is determined to be $a^\mu = (+0.11 \pm 0.03)\%$.

Possible pion reconstruction asymmetries are studied using $K^0_S \to \pi^+\pi^-$ and $K^{\pm *} \to K^0_S\pi^\pm$ decays in data, in addition to the use of dedicated simulations. No significant asymmetry is observed in any case, and the pion correction a^π is taken to be zero. A systematic uncertainty of ±0.05% is allocated to account for the limited precision on this quantity.

8. Sample Composition: $F^{\rm osc}_{B^0_{(s)}}$

Not all $\mu D_{(s)}$ combinations originate from the decay of oscillated $B^0_{(s)}$ mesons. Alternative charge symmetric sources will contribute only to the denominator in the raw asymmetry extraction, and hence dilute any physical asymmetry $a^q_{\rm sl}$. The total fraction of signal events arising from $B^0_{(s)}$ meson decays is determined using inclusive MC simulations in which the only requirement at the generator level is the presence of the appropriate $D^{(*)\mp}_{(s)}$ decay channel, and the presence of a muon (of any charge). The parentage information is then extracted from these signal samples. Oscillations are simulated by weighting each signal MC event j according to the appropriate dependence on its decay time t, by a factor

$$W^{\rm mix}_j = \frac{1}{2}[1 - \cos(\Delta M_q \cdot t_j)]. \qquad (14)$$

The dilution factor for B^0 mesons $F^{\rm osc}_{B^0}$ is then the sum of all MC weights $W^{\rm mix}_j$ in the appropriate VPDL bin, divided by the total MC event count for that bin. Any $\mu D^{(*)}$ candidates from non B^0 decays are assigned a weight of zero. For B^0_s mesons, the analogous procedure is followed, but without VPDL binning. Possible asymmetry contributions from B^0 decays in the B^0_s sample, and vice versa, are taken into account, but found to be negligible. The results for both B^0 channels are shown in Table 1, demonstrating the progressive increase in the fraction of oscillated mesons as the VPDL increases. For the B^0_s case, the single dilution fraction is determined to be $F^{\rm osc}_{B^0_s} = 0.465 \pm 0.017$, accounting for the fact that around 93% of the μD_s candidates are from B^0_s decay, and almost exactly 50% of these oscillate prior to decay. Systematic uncertainties are allocated to account for the limited knowledge of the decay branching ratios of B mesons, and for the finite precision on the lifetimes and mixing frequencies. The statistical uncertainty from the MC samples is also catagorised as systematic for the final measurement.

9. Results

From the raw asymmetries, detector-related asymmetries, and the dilution fractions $F^{\rm osc}_{B^0_{(s)}}$, the final value of the semileptonic mixing asymmetry $a^d_{\rm sl}$ is determined for each VPDL bin and for both channels, as presented in Table 1. The first two VPDL bins are not included, as these represent the control region in which the expected signal contribution is negligible. These results can be combined by weighted average, firstly into two channel-specific measurements:

$$\begin{aligned} a^d_{\rm sl}(\mu D) &= [0.43 \pm 0.63\ (\text{stat.}) \pm 0.16\ (\text{syst.})]\%, \\ a^d_{\rm sl}(\mu D^*) &= [0.92 \pm 0.62\ (\text{stat.}) \pm 0.16\ (\text{syst.})]\%, \end{aligned}$$

and finally into a single measurement:

$$a^d_{\rm sl} = [0.68 \pm 0.45\ (\text{stat.}) \pm 0.14\ (\text{syst.})]\%.$$

Correlations between uncertainties are properly accounted for in these combinations. The resulting precision is dominated by limited statistics in the signal channel, and is better than the current world-average precision obtained by combining results from the B factories.

The corresponding single measurement in the B^0_s channel is

$$a^s_{\rm sl} = [-1.12 \pm 0.74\ (\text{stat.}) \pm 0.17\ (\text{syst.})]\%.$$

This is significantly more precise than the previous best measurement of this parameter. In both cases, the measured asymmetries are consistent with the SM prediction, and also with the equivalent measurements from the D0 dimuon asymmetry analysis.

Various cross-checks of the analysis procedure are made, including repeating the measurements with the data divided into orthogonal pairs of sub-samples. The division criteria include low/high momentum candidates, forward/central candidates, forward/backward candidates, different run periods, and different quality of tracks. In all cases, the variations between samples are completely consistent with statistical fluctuations.

Additional details are available for the $a^d_{\rm sl}$ measurement in Ref. [13], and for the $a^s_{\rm sl}$ measurement in Ref. [14].

References

[1] A. D. Sakharov, Pisma Zh. Eksp. Teor. Fiz. **5**, 32 (1967) [JETP Lett. **5**, 24 (1967)] [Sov. Phys. Usp. **34**, 392 (1991)].

[2] J. Beringer *et al.* (Particle Data Group), Phys. Rev. D **86**, 010001 (2012), and `http://www.slac.stanford.edu/xorg/hfag/osc/spring_2012/`.

[3] P. Huet and E. Sather, Phys. Rev. D **51**, 379 (1995)

[4] A. Lenz and U. Nierste, J. High Energy Phys. **07**, 072 (2007) (and recent update arXiv:1102.4274 [hep-ph]).

[5] A. Lenz, U. Nierste, J. Charles, S. Descotes-Genon, A. Jantsch, C. Kaufhold, H. Lacker, S. Monteil, V. Niess and S. T'Jampens, Phys. Rev. D **83**, 036004 (2011).

[6] V. M. Abazov *et al.* [D0 Collaboration], Phys. Rev. D **82**, 012003 (2010) [Erratum-ibid. D **83**, 119901 (2011)] [arXiv:0904.3907 [hep-ex]].

[7] V. M. Abazov *et al.* (D0 Collaboration), Phys. Rev. D **84**, 052007 (2011).

[8] V. M. Abazov *et al.* (D0 Collaboration), Phys. Rev. D **85**, 032006 (2012).

[9] T. Aaltonen *et al.* (CDF Collaboration), Phys. Rev. D **85** 072002 (2011); arXiv:1208.2967 [hep-ex], submitted to Phys. Rev. Lett. (2012).

[10] R. Aaij *et al.* (LHCb Collaboration), Phys. Rev. Lett. **108**, 101803 (2012).

[11] A. Lenz, U. Nierste, J. Charles, S. Descotes-Genon, H. Lacker, S. Monteil, V. Niess and S. T'Jampens, arXiv:1203.0238 [hep-ph].

[12] V.M. Abazov *et al.* (D0 Collaboration), Nucl. Instrum. Methods Phys. Res. A **565**, 463 (2006).

[13] V. M. Abazov *et al.* (D0 Collaboration), arXiv:1208.5813v1 [hep-ex], submitted to Phys. Rev. D (2012).

[14] V. M. Abazov *et al.* (D0 Collaboration), arXiv:1207.1769v1 [hep-ex], submitted to Phys. Rev. Lett. (2012).

[15] V. M. Abazov *et al.* (D0 Collaboration), Phys. Rev. D **82**, 032001 (2010).